Available online at www.sciencedirect.com

SCIENCE DIRECT®

Estuarine, Coastal and Shelf Science 57 (2003) 929–940

ESTUARINE
COASTAL
AND
SHELF SCIENCE

Effect of emersion and immersion on the porewater nutrient dynamics of an intertidal sandflat in Tokyo Bay

Tomohiro Kuwae[a,*], Eiji Kibe[b], Yoshiyuki Nakamura[a]

[a]Coastal Ecosystems Division, Port and Airport Research Institute, 3-1-1, Nagase, Yokosuka 239-0826, Japan
[b]Karatsu Port Construction Office, Ministry of Land, Infrastructure and Transport, 3-216-1, Futago, Karatsu, Saga 847-0861, Japan

Received 22 January 2002; accepted 20 November 2002

Abstract

Porewater nutrient dynamics during emersion and immersion were investigated during different seasons in a eutrophic intertidal sandflat of Tokyo Bay, Japan, to elucidate the role of emersion and immersion in solute transport and microbial processes. The water content in the surface sediment did not change significantly following emersion, suggesting that advective solute transport caused by water table fluctuation was negligible. The rate of change in nitrate concentration in the top 10 mm of sediments ranged from -6.6 to 4.8 μmol N l^{-1} bulk sed. h^{-1} during the whole period of emersion. Steep nutrient concentration gradients in the surface sediment generated diffusive flux of nutrients directed downwards into deeper sediments, which greatly contributed to the observed rates of change in porewater nutrient concentration for several cases. Microbial nitrate reduction within the subsurface sediment appeared to be strongly supported by the downward diffusive flux of nitrate from the surface sediment. The stimulation of estimated nitrate production rate in the subsurface layer in proportion to the emersion time indicates that oxygenation due to emersion caused changes in the sediment redox environment and affected the nitrification and/or nitrate reduction rates. The nitrate and soluble reactive phosphorus pools in the top 10 mm of sediment decreased markedly during immersion (up to 68% for nitrate and up to 44% for soluble reactive phosphorus), however, this result could not be solely explained by molecular diffusion.

Keywords: interstitial nutrients; microbial processes; diffusive fluxes; oxygenation; nitrogen and phosphorus cycles; eutrophication; Banzu tidal flat

1. Introduction

Semi-diurnal movement of tidal water alters biotic and abiotic environments in intertidal sediments over short time intervals (Alongi, 1998). When sediments are exposed to air, the water table drops due to drainage and evaporation (Agosta, 1985; Anderson & Howell, 1984; Howes & Goehringer, 1994). During tidal flooding, in turn, vertical infiltration of tidal water controls interstitial water levels (Hemond & Fifield, 1982). Rhythmic emersion and immersion can also mediate the below-ground transport of nutrients and metabolic products (Dolphin, Hume, & Parnell, 1995; Harvey & Odum, 1990). The role of advective solute transport in the distribution of nutrients has mainly been reported for salt marsh creekbanks (e.g. Agosta, 1985; Howes & Goehringer, 1994; Yelverton & Hackney, 1986) and sandy beaches (McLachlan & Illenberger, 1986; Uchiyama, Nadaoka, Rölke, Adachi, & Yagi, 2000). In contrast, the movement of water and solutes associated with a fall in the water table has been reported to be minor in non-vegetative intertidal flats due to the development of a capillary fringe (Drabsch, Parnell, Hume, & Dolphin, 1999).

The biogeochemistry of intertidal sediments during immersion has been well studied in relation to the sediment–water column exchange of nutrients (e.g. Asmus et al., 1998; Cabrita & Brotas, 2000; Falcão & Vale, 1990, 1998; Kuwae, Hosokawa, & Eguchi, 1998; Middelburg, Klaver, Nieuwenhuize, & Vlug, 1995; Mortimer et al., 1999). However, little is yet known of

---

* Corresponding author.
E-mail address: kuwae@ipc.pari.go.jp (T. Kuwae).

0272-7714/03/$ - see front matter © 2003 Elsevier Ltd. All rights reserved.
doi:10.1016/S0272-7714(02)00423-7

the dynamics of porewater nutrients in such sediments during emersion or transitional periods (Rocha, 1998; Rocha & Cabral, 1998; Usui, Koike, & Ogura, 1998). During emersion, the penetration of oxygen into sediments may increase (Brotas, Amorim-Ferreira, Vale, & Catarino, 1990), causing changes in the redox environment (Koch, Maltby, Oliver, & Bakker, 1992). This oxygenation affects the rates and pathways of nutrient flow (Kerner, 1993) related to, e.g. aerobic nitrifiers and anaerobic denitrifiers (Henriksen & Kemp, 1988; Parkin, 1990; Seitzinger, 1988). In addition, the absence of overlying waters indicates no efflux of nutrients from the sediment, which will either accumulate or be consumed within the sediments. Rocha (1998) has shown that total (dissolved and exchangeable) sedimentary ammonium accumulated during emersion. Usui et al. (1998) have reported that porewater nitrate decreased remarkably during the initial 3–4 h after the onset of emersion. On the other hand, at immersion, mixing of porewater with overlying water can result in drastic changes in the interstitial nutrient pool (Rocha, 1998; Rocha & Cabral, 1998). Rocha and Cabral (1998) have shown that approximately 80% of the nitrate pool was flushed during immersion.

This paper reports the dynamics of porewater nutrients induced by tidal cycles in a eutrophic intertidal sandflat of Tokyo Bay, Japan. To our knowledge, this is the first report dealing with tide-induced temporal changes in the concentrations of three porewater nutrient species (nitrate, ammonium, and soluble reactive phosphorus) during different seasons. Special emphasis is placed on (1) the influence of diffusive fluxes and advective transport on the pool size of nutrients during emersion and immersion; and (2) the role of emersion in the microbial processes, which affect porewater nutrient concentration.

2. Materials and methods

2.1. Study site

The Banzu intertidal sandflat is located on the east coast of Tokyo Bay (Japan) and covers an area of 7.6 km^2 (Fig. 1). Tokyo Bay receives a nutrient loading from a population of ca. 26 million humans (320 t N day^{-1} for total nitrogen and 26 t P day^{-1} for total phosphorus, Nakanishi, 1993), and is subjected to heavy eutrophication and anoxia in bottom waters over a wide area during the summer. Tides are semi-diurnal with amplitudes from 0.5 to 1.6 m (Guo & Yanagi, 1994). The Obitsu River has a watershed area of 267 km^2 and 2.5–3.0 m^3 s^{-1} of normal discharge. The sampling site (35° 24.2′N, 139°54.2′E) is 30 cm above mean sea level,

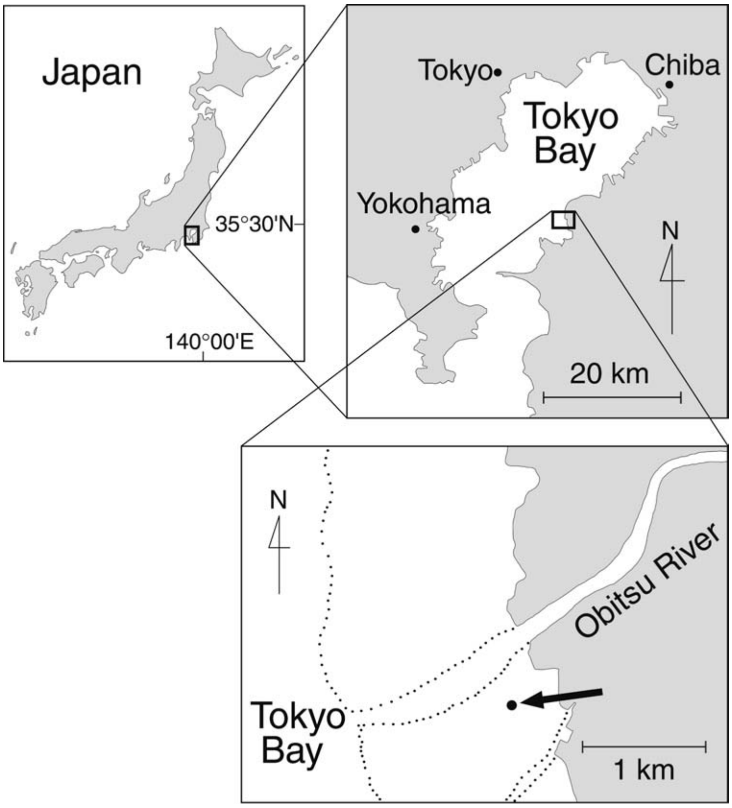

Fig. 1. Location of the study site (Banzu intertidal sandflat, Tokyo Bay). Dotted line indicates the lowest tidal level.

experiencing emersion and immersion during each tidal phase. The slope of the seabed at the sampling site is very low (0.07 cm m^{-1}). Sediments are characterized by well-sorted fine sand (99.6% sand and 0.4% silt) with a median grain size of 170 µm (Kuwae & Hosokawa, 1999). Organic carbon and total nitrogen contents at 0–20 mm depth, measured from August 1998 to September 1999, were 0.981 ± 0.047 mg C g^{-1} dry wt. (mean ± SE, $n = 45$) and 0.214 ± 0.013 mg N g^{-1} dry wt. (mean ± SE, $n = 45$), respectively. There is no macro-vegetation, and pennate diatoms dominate the epibenthic microalgal flora. Gross primary production in September 1997, measured by sediment core incubation under both light and dark conditions was 151.9 ± 17.1 mg O_2 m^{-2} h^{-1} (mean ± SE, $n = 3$) (Kuwae et al., 1998).

We conducted four seasonal surveys on the spring tide: March 1998, May 1998, September 1998, and November 1998. One tidal cycle was sampled in each survey. The tidal range on the survey days ranged from 1.1 to 1.6 m. No rainfall was recorded during surveys of the tidal flat.

2.2. Hydrology

To track fluctuations in the water table depth, a small well was dug into the sediment a few days before each survey. A polyvinyl chloride pipe (4.5 cm internal diameter (i.d.)), with holes drilled and covered with a nylon mesh, was placed in the well to a depth of 25 cm. Water levels in the pipe were measured using a float.

The diffusive flux of nutrients from the sediment during immersion was calculated according to Fick's first law of diffusion (Berner, 1980):

$$J = -\varphi D_S (\mathrm{d}C/\mathrm{d}x),$$

where J is the diffusive efflux, φ is the porosity at the sediment surface (0–10 mm), x is the vertical axis and D_S is the whole sediment diffusion coefficient. D_S was calculated from the temperature corrected diffusion coefficient in particle-free water (D_0) (Li & Gregory, 1974) and tortuosity reported by Sweerts, Kelly, Rudd, Hesslein, and Cappenberg (1991). $\mathrm{d}C/\mathrm{d}x$ is the concentration gradient across the sediment–water interface. $\mathrm{d}C/\mathrm{d}x$ was calculated by linear interpolation between the overlying water concentration at the sediment surface and the porewater concentration in the 0–2.5 mm section assigned to 1.25 mm depth.

2.3. Sediment characteristics

At each survey, the photon flux of photosynthetically available radiation (PAR), sediment temperature, redox potential (Eh), porosity, water content, chlorophyll *a*, and macrofauna were measured. PAR was continuously measured during each sampling time using a Biospherical quantum sensor. Sediment temperature and Eh were measured in situ at intervals of 2–5 cm during emersion using a temperature probe (RT-10; Tabai Espec) and a platinum redox electrode (HM-14P; TOA). For the measurement of porosity and water content, core samples were taken to a depth of 1 cm with acrylic tubes (4.5-cm i.d.) during both emersion and immersion. Porosity and water content were determined by the weight loss after drying wet sediments at 90 °C for 24 h. The remainder of each emersion period core sample was used for the analysis of chlorophyll *a* in the sediment, extracted using 90% acetone solution, spectrophotometrically analyzed (U-3200; Hitachi) according to Lorenzen (1967). For the measurement of macrofaunal abundance, core samples ($n = 8$) were taken to a depth of 20 cm with acrylic tubes (25 cm long × 8.6 cm i.d.). The sediment in each core was sieved (1 mm mesh) to retain macrofauna. Macrofauna were preserved in neutralized 10% formalin–seawater solution and stored for later counting.

2.4. Porewater solutes

On each survey day, sediment samples were taken every one to several hours from the onset of emersion to after immersion. Sediment cores ($n = 3$) were collected randomly from the site (2 m × 2 m) at each sampling, using an acrylic corer (8.6 cm i.d. × 25 cm long). Sediment cores were immediately cut in situ into 2.5–10 mm segments, and macrofauna were removed from sliced sediments. The sliced sediments were immediately fixed by dried ice in order to stop biogeochemical reactions. Fixed sediments were thawed and filled in syringes (10 ml) and were centrifuged for 10 min at 2000 rpm ($580 \times g$) at ambient temperature. Extracted water was filtered through a Millipore HA filter. Filtered water was immediately frozen for the later analysis of nutrients and salinity. Ammonium, nitrate, nitrite, and soluble reactive phosphorus (SRP) were measured using standard colorimetric techniques (Strickland & Parsons, 1972) on an analyzer (TRAACS-800; Bran + Luebbe). Salinity was measured using a conductivity electrode (9382-10D; Horiba).

2.5. Statistical analysis

Linear regression was used to calculate the rate of change in porewater nutrient concentrations over the whole period of emersion. A one-way ANOVA was used to examine statistical differences in porewater nutrient concentrations between the last samples collected before immersion and the first samples collected after immersion. Data sets were tested for homogeneity of variances (Hartley test), and the log-transformed values were used if needed for a normal distribution.

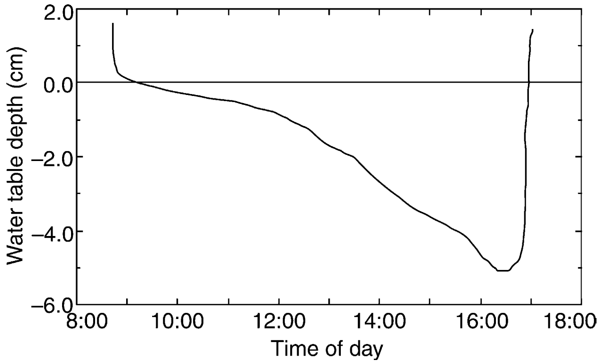

Fig. 2. Representative data (May 1998) for the fall and rise of water table depth (cm) measured by using a small well during emersion.

3. Results

3.1. Water table dynamics

The sediment water table was measured by using a well dropped gradually following emersion (Fig. 2). Slightly before the onset of the next immersion, the water table dropped to its lowest level, and then rose steeply. This pattern was observed for all cases (not shown). The greatest water table drop (7.8 cm) occurred in summer (September 1998), and the smallest (2.7 cm) in winter (March 1998).

3.2. Sediment characteristics

The sampling days of March 1998 and May 1998 were cloudy, showing low PAR averages during the sampling time; the remainder showed high PAR values (Table 1). During emersion, Eh was >0 mV for all seasons and depths, except below 5 cm in summer, when the mean sediment temperature in the top 10 cm reached a maximum (30.1 °C) (Fig. 3). Although there was a measurable decline in the water table level during emersion, no statistical differences in the water content and porosity were observed between emersion and immersion for any season ($P > 0.05$) (Table 1). Within the samples studied, the porosity and water content ranged from 44.6 ± 0.4 to 47.7 ± 1.0% (mean ± SE) and 23.6 ± 0.3 to 25.9 ± 0.8% (mean ± SE), respectively. Salinity of the porewater was close to that of tide water. The porewater salinity never varied more than 3.0 from the tide (surface) water salinity during the study. This strongly suggests that there was no significant ground water input. The chlorophyll *a* content in the top 10 mm of sediments ranged from 1.15 ± 0.16 to 8.33 ± 0.68 μg cm^{-3} (mean ± SE) (Table 1). The polychaete *Armandia* sp. and the bivalve *Ruditapes philippinarum* dominated infauna, whereas the gastropod *Batillaria cumingii* dominated epifauna (Table 2).

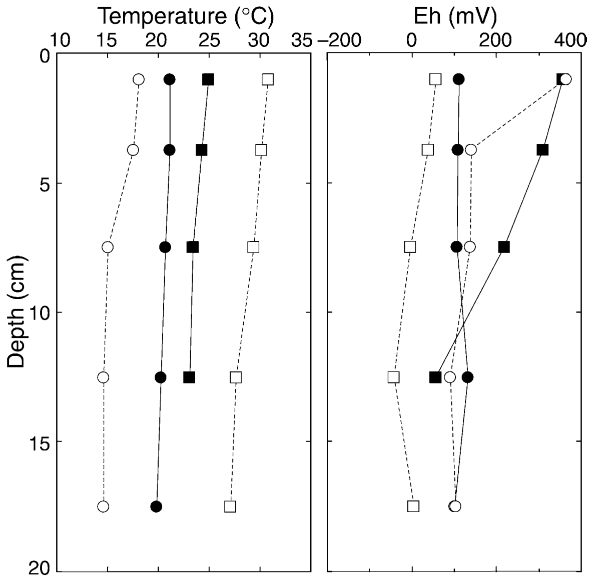

Fig. 3. Vertical profiles of sedimentary temperature (°C) and redox potential (mV) during emersion. Seasons: March 1998 (○); May 1998 (●); September 1998 (□); and November 1998 (■).

3.3. Porewater nutrient profiles

Depth profiles of porewater nitrate + nitrite (hereafter, nitrate) and SRP during emersion showed marked concentration gradients with depth (Fig. 4); nitrate and SRP concentrations peaked in the uppermost layer of sediments for all the seasons, and below this they sharply declined until a depth of 30 mm. Nitrate concentrations in the upper layer peaked in November 1998

Table 1
Sediment water content during emersion and immersion, sediment chlorophyll *a* content, and photosynthetically available radiation (PAR) during sampling time

	Water content (%)[a]			
	Emersion[b]	Immersion[c]	Chlorophyll *a*[a] (μg cm^{-3})	PAR (μmol m^{-2} s^{-1})
March 1998	25.9 ± 0.8	24.7 ± 0.4	1.15 ± 0.16	108
May 1998	24.8 ± 0.2	24.4 ± 0.4	4.49 ± 1.08	152
September 1998	23.7 ± 0.3	24.1 ± 0.4	5.68 ± 0.41	639
November 1998	24.6 ± 0.2	23.6 ± 0.3	8.33 ± 0.68	499

[a] Measured by using 0–10 mm depth sediments and are given as mean ± SE ($n = 3$).
[b] Samples were taken ca. 1 h before immersion.
[c] Samples were taken ca. 1 h after immersion.

Table 2
Total densities (mean ± SE) and dominant species of macrofauna (>10%) at the sampling site (depth: 0–20 cm)

		Dominated macrofauna		
	Total (individuals m^{-2})	Species	Individuals m^{-2}	%
March 98	1657 ± 232	*Armandia* sp.	796 ± 172	48.1
		Ceratonereis erythraeensis	560 ± 96	33.8
May 98	689 ± 239	*Pseudopolydora* sp.	495 ± 182	71.9
		Ruditapes philippinarum	194 ± 89	28.1
September 98	3658 ± 753	*Armandia* sp.	2044 ± 505	55.9
		Batillaria cumingii	603 ± 138	16.5
		Ruditapes philippinarum	495 ± 100	13.5
		Decorifer insignis	452 ± 200	12.4
November 98	3163 ± 187	*Armandia* sp.	1184 ± 110	37.4
		Batillaria cumingii	753 ± 134	23.8
		Decorifer insignis	581 ± 117	18.4
		Ruditapes philippinarum	517 ± 103	16.3

and were minimal in September 1998. Ammonium profiles either exhibited a stable pattern, or a gradual decrease in concentration from the sediment–water interface. All the nutrient concentrations in the uppermost sediments, except for nitrate in September 1998, were always higher than those in overlying waters.

3.4. Nutrient dynamics during emersion

Remarkable changes in nitrate and SRP concentrations in the upper layers were observed during emersion, whereas deeper layers (>10 mm) showed only slight changes (Fig. 4). A linear regression analysis revealed that the rates of change in nitrate concentration during emersion were statistically significant ($P < 0.05$) for most samples of the top 10 mm sediments, ranging from −6.6 to 4.8 μmol N l^{-1} bulk sed. h^{-1} (Fig. 5). These rates were positive in May 1998, negligible in March 1998, and negative in both September 1998 and November 1998. However, the rates of change in nitrate concentration approached zero below 20 mm depth. Ammonium concentration decreased with time, except for the summer samples, where they increased (Fig. 4). The rates of change in ammonium concentration were near constant with depth, in contrast to the rates measured for other nutrient species (Fig. 5). The maximum rate of decrease in ammonium concentration (−22.9 μmol N l^{-1} bulk sed. h^{-1}) was observed in the deeper layer (20–25 mm) in spring, whereas the maximum rate of increase (11.8 μmol N l^{-1} bulk sed. h^{-1}) was observed in the deepest layer (90–100 mm) in summer (not shown). Few statistically significant rates of change in SRP concentration were measured (Fig. 5); the greater changes were observed in the upper layers than in the deeper layers (>30 mm).

3.5. Nutrient dynamics at immersion

Nitrate and SRP concentrations in the top layers showed marked changes at immersion as well as during emersion, except for November 1998 samples (Fig. 4). In general, the concentrations of nitrate and SRP in the top 10 mm layers showed decreasing trends at immersion although few cases exhibited statistically significant differences (Fig. 6). These declines resulted in loss of the nitrate pool (−4 to 68%, mean: 32.8%) and the SRP pool (−4 to 44%, mean: 20.8%) in the top 10 mm of sediments. The patterns of change in ammonium concentration were constant with depth except for those measured in May 1998 (Fig. 6).

4. Discussion

4.1. Porewater hydrology

The water content of the Banzu intertidal surface sediment did not change significantly following emersion although a measurable fluctuation was observed for the water table depth (where pore pressure equals atmospheric pressure) (Fig. 2). This could be attributed to the development of a capillary fringe above the water table depth (where pore pressure is less than atmospheric pressure) and a high moisture retention capacity at the top of the sandy sediments (Drabsch et al., 1999) (Fig. 7). Hence, interstitial water and solutes were probably held at the surface during emersion and little transport occurred into deeper sediments. Drabsch et al. (1999) found that the water table fell only a few centimeters below the sediment surface of an intertidal sandflat in Manukau Harbour, New Zealand, and the top of the sediments remained close to saturation throughout the tidal cycle. Hemond and Fifield (1982) examined the hydrological regime in a peaty, New England marsh and found seepage rates to be low, and also found that sediments remained saturated throughout the tidal cycle. In contrast, emersion of intertidal areas resulted in surface sediment water contents decreasing by 3.5% at Tama estuary in Tokyo Bay (Usui et al., 1998), and by more than 10% in Sado estuary (Rocha, 1998). The main

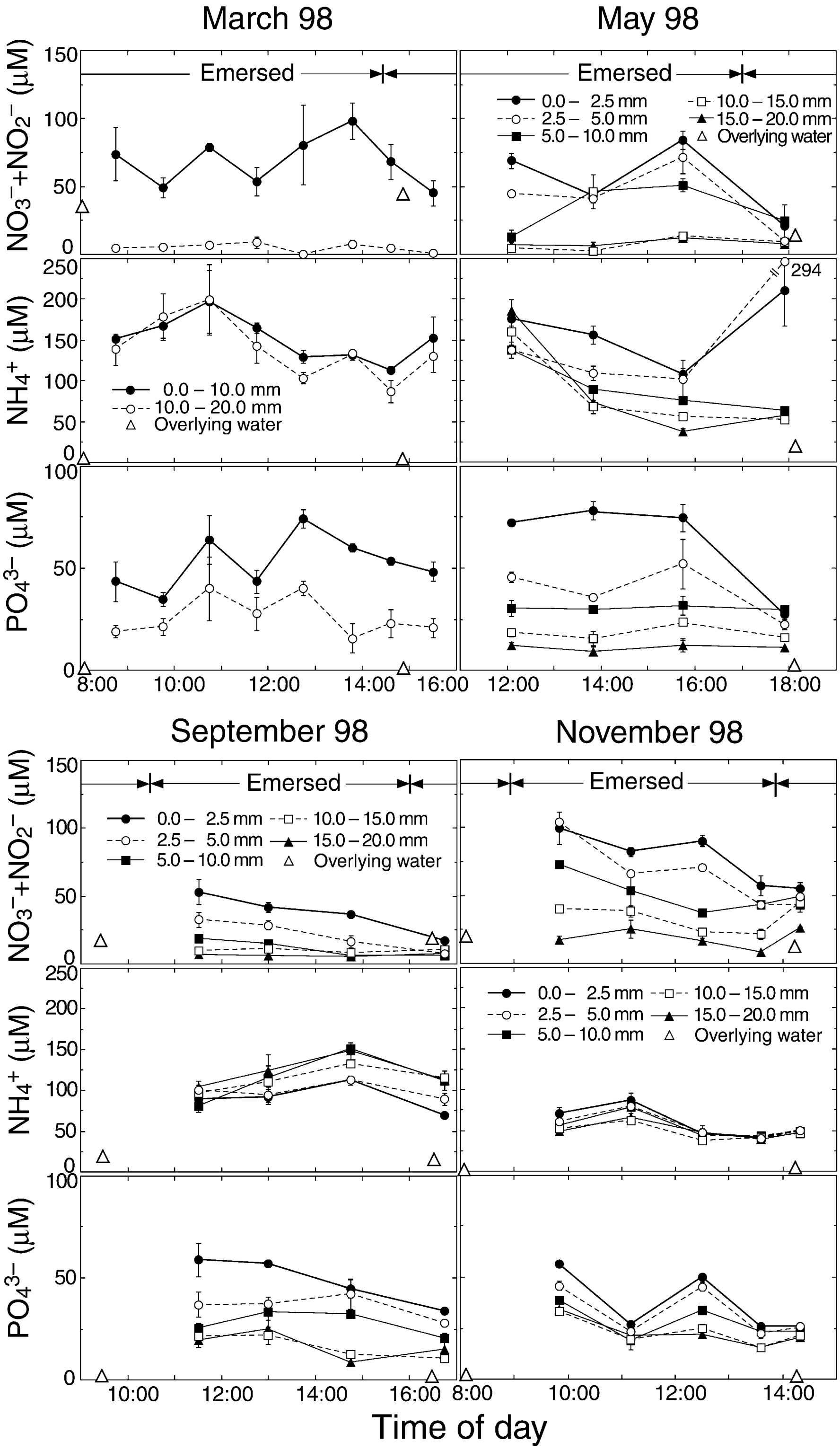

Fig. 4. Temporal changes in interstitial nutrient concentrations (μM). Error bars indicate standard errors ($n = 3$). Only data from the top 20 mm sediment are shown to improve clarity. Note that the depth interval for March 98 is different from the other seasons.

reason for the discrepancy in water content dynamics during emersion between sites is probably due to differences in the length of emersion time, topographical slope, and substrate type (permeability). It is also possible that porewater around large macrobenthic burrows is more mobile (Allanson, Skinner, & Imberger, 1992), and therefore independent of capillary fringe processes. This greater fluid channeling through burrows

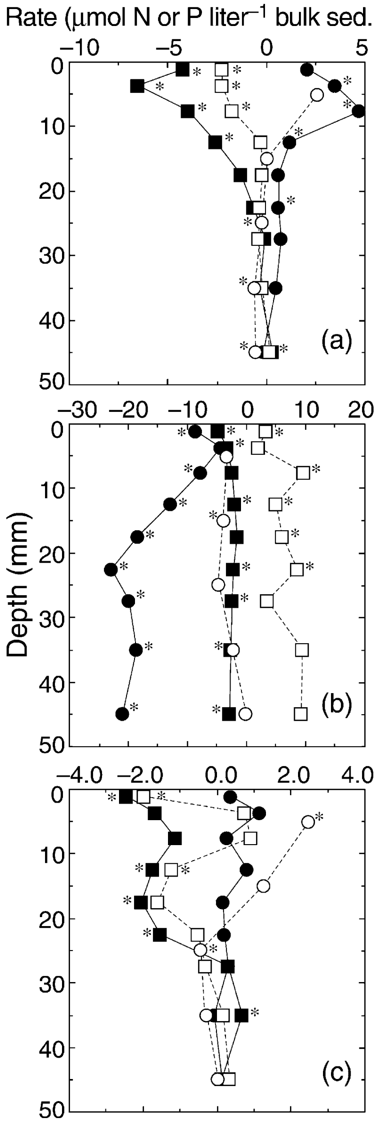

Fig. 5. Rates of change in interstitial nitrate + nitrite (a), ammonium (b), and SRP (c) concentrations (μmol N or P l^{-1} bulk sed. h^{-1}) during the whole period of emersion. Seasons: March 1998 (○); May 1998 (●); September 1998 (□); and November 1998 (■). The rates were calculated using a linear regression analysis. Plots with asterisks indicate statistically significant rates of change at the 5% level.

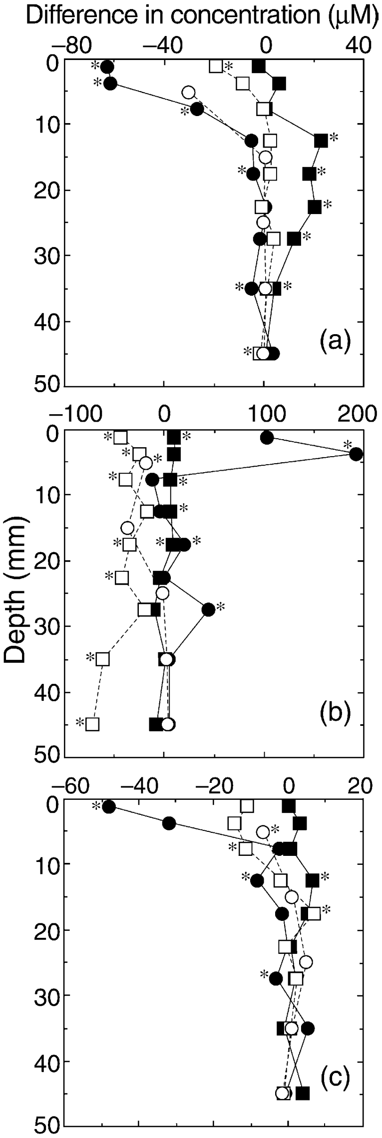

Fig. 6. Differences in interstitial nitrate + nitrite (a), ammonium (b), and SRP (c) concentrations (after immersion–before immersion) (μM). Seasons: March 1998 (○); May 1998 (●); September 1998 (□); and November 1998 (■). Plots with asterisks indicate statistically significant differences in concentration at the 5% level using a one-way ANOVA ($n = 3$).

may influence nutrient dynamics. Nevertheless, during emersion, the influence of advection on porewater nutrient dynamics is minor at our site.

4.2. Effect of diffusive fluxes and production during emersion

The porewater hydrology described above shows that all spatial transport of solutes in the sediment is assumed to have taken place by one-dimensional diffusion, i.e., both horizontal and vertical advections caused by hydraulic gradients or water table movement, can be neglected. Therefore, the observed rate of change in porewater nutrient concentration should be governed by molecular diffusive transport and production:

$$\varphi \frac{\partial C}{\partial t} = \varphi D_S \frac{\partial^2 C}{\partial x^2} + P,$$

where C is the concentration of the nutrient species in the porewater, t the time, x the depth, and P is the rate of production or consumption of the nutrient species per unit volume of sediment. The porosity (φ) and the whole sediment diffusion coefficient (D_S) were assumed to be constant with depth and time. Data shown in Fig. 5 were used for the left hand. The first right-hand term is the diffusive flux contribution per unit volume of sediment

Fig. 7. Condition of the surface sediment ca. 30 min before immersion. The sediment remained saturated.

as described by Fick's second law of diffusion (Berner, 1980). The diffusive flux contribution was calculated for each sampling time during emersion and then averaged. Using this equation, *P* was estimated for each nutrient species and each depth.

Table 3 shows that several diffusive fluxes of nutrient species during emersion contributed greatly to the observed rate of change in the porewater nutrient concentration of the surface sediment (0–10 mm). The influence of diffusive flux is less for the subsurface layer (10–40 mm). This reflects steeper nutrient concentration gradients in the near-surface compared to the deeper environment (Fig. 4).

The range of the estimated production rates were: (1) nitrate: -4.9 to $5.5\,\mathrm{mmol\,N\,m^{-3}}$ bulk sed. $\mathrm{h^{-1}}$; (2) ammonium: -18.6 to $9.4\,\mathrm{mmol\,N\,m^{-3}}$ bulk sed. $\mathrm{h^{-1}}$; and (3) SRP: -1.9 to $2.6\,\mathrm{mmol\,P\,m^{-3}}$ bulk sed. $\mathrm{h^{-1}}$ (Table 3). Obviously, much higher nitrate concentrations in the surface sediment than in the overlying water (Fig. 4) indicate a high nitrification activity in the Banzu intertidal flat sediment. Moreover, in situ nitrification rates are likely to be higher than the estimated nitrate production rates, which may include microbial nitrate reduction as well as nitrification. Nevertheless, in general, only the topmost layer showed nitrate production, being the main site of nitrification (Koike & Sørensen, 1988). Nitrate in the 2.5–10.0 mm sediment was supplied through molecular diffusion from the topmost layer (0–2.5 mm) and was largely consumed within this layer. This indicates that microbial nitrate reduction within the subsurface sediment, including denitrification and dissimilatory ammonification (Fenchel, King, & Blackburn, 1998), is strongly supported by diffusive influx of nitrate from the surface sediment,

Table 3
Observed rate of change in porewater nutrient concentration (Obs), diffusive flux contribution (Diff), and rate of nutrient production (Prod) during emersion

		$NO_3^- + NO_2^-$			NH_4^+			PO_4^{3-}		
	Depth (mm)	Obs[a,b]	Diff[a,c]	Prod[a,d]	Obs	Diff	Prod	Obs	Diff	Prod
March 1998	0–10	2.6	−1.0	3.6	−3.3	−0.2	−3.1	2.5	−0.1	2.6
	10–40	−0.3	0.3	−0.6	−4.0	0.0	−4.0	0.2	0.0	0.2
May 1998	0–2.5	2.0	−3.5	5.5	−8.7	−11.2	2.5	0.4	−2.0	2.4
	2.5–5.0	3.5	1.3	2.2	−4.4	9.5	−13.9	1.1	1.6	−0.5
	5.0–10	4.8	−0.5	5.3	−7.8	0.9	−8.7	0.3	0.0	0.3
	10–40	0.7	0.3	0.4	−18.6	0.0	−18.6	0.3	0.0	0.3
September 1998	0–2.5	−2.3	−4.9	2.6	3.3	2.0	1.3	−2.0	−2.2	0.2
	2.5–5.0	−2.3	2.3	−4.6	1.9	−1.8	3.7	0.7	1.7	−1.0
	5.0–10	−1.8	0.8	−2.6	9.7	0.3	9.4	0.9	0.1	0.8
	10–40	−0.4	0.1	−0.5	6.4	0.0	6.4	−0.7	0.0	−0.7
November 1998	0–2.5	−4.4	−3.0	−1.4	−4.8	−1.6	−3.2	−2.5	−0.6	−1.9
	2.5–5.0	−6.6	−1.8	−4.8	−3.5	1.0	−4.5	−1.7	0.1	−1.8
	5.0–10	−4.0	0.9	−4.9	−2.6	−0.3	−2.3	−1.1	0.1	−1.2
	10–40	−1.0	0.3	−1.3	−2.2	0.1	−2.3	−0.9	0.0	−0.9

[a] All values are in mmol N or P $\mathrm{m^{-3}}$ bulk sed. $\mathrm{h^{-1}}$. All values for the 10–40 mm depth were averaged (March 1998: $n = 3$; others: $n = 6$).
[b] Same data as Fig. 5.
[c] Calculated using Fick's second law of diffusion. Negative values indicate loss of nutrients.
[d] Estimated as: Obs–Diff. negative values of Prod indicate the consumption of nutrients.

where nitrification activity is high. Supply of high concentrations of nitrate into deeper layers during emersion may support some stocks of nitrate and the stimulation of deeper layer denitrification (Alongi, Tirendi, Dixon, Trott, & Brunskill, 1999). Alongi et al. (1999) speculated that the rapid denitrification rates measured for intertidal mudflat and mangrove forest sediments reflect a vertically expanded zone of denitrification caused by the presence of nitrate in deeper sediments.

In summer, the rate of estimated ammonium production was stimulated for all of the sediment layers (Table 3); this coincided with the highest observed temperatures (Fig. 3). Estimated ammonium production processes probably include dissimilatory ammonium production and mineralization. Temperature dependence of benthic mineralization has been observed for various shallow environments (e.g. Jørgensen & Sørensen, 1985; Middelburg et al., 1996; Trimmer, Nedwell, Sivyer, & Malcolm, 2000). In addition, low Eh within the deeper layers (Fig. 3) is an evidence of anaerobic decomposition of accumulated organic matter. Dissimilatory ammonium production in the deeper layers was probably only a minor contributor to total estimated ammonium production due to low nitrate concentrations (Fig. 4).

We plotted the estimated production rates of nitrate and ammonium versus the emersion time of the sediment in order to investigate if emersion-related oxygenation influences production rates in the subsurface layer (2.5–10 mm) (Fig. 8). The rate of estimated nitrate production was stimulated in proportion to the emersion time ($r = 0.80$, $P = 0.029$) although no statistically significant relationship was found between the rate of estimated ammonium production and the emersion time ($r = 0.51$, $P = 0.240$). These relationships indicate a weakening of the anoxic environment by oxygenation during emersion, and subsequent (1) stimulation of nitrification; or (2) inhibition of nitrate reduction; or (3) a combination of both processes. With regard to this emersion-related oxygenation, Koch et al. (1992) found that Eh increased during emersion of mudflat subsurface sediments (3–5 mm) in River Torridge, England. Our observed relationship between the rate of estimated nitrate production and the emersion time is consistent with nitrate behavior in Tama estuary sediments, Japan, where the nitrate pool was constant or slightly increased 3–4 h after the onset of emersion (Usui et al., 1998).

Understanding the other mechanisms affecting porewater nutrient concentration needs further investigation. For instance, porewater nutrients can be assimilated by microphytobenthos during emersion as well as during immersion because of their high levels of productivity at the site (Kuwae et al., 1998). The decrease in SRP concentration on sunny days of September 1998 and November 1998 (Table 1; Fig. 4) might support the active microalgal photosynthesis and the following uptake of SRP from porewater during emersion. Diurnal variation in nitrification and denitrification can also mediate the pool size of nutrients (Ottosen, Risgaard-Petersen, Nielsen, & Dalsgaard, 2001). Using a new ^{15}N-ammonium spray technique, Ottosen et al. (2001) demonstrated that coupled nitrification–denitrification rates during the day were lower than at night in exposed intertidal mudflats of the Tagus estuary. As for the depth profile of nutrients, the effect of infaunal bioturbation may be important for our site because the dense population of the polychaetes *Armandia* sp. and *Pseudopolydra* sp. was observed (Table 2). Sediment reworking by these animals can stimulate the homogenization of nutrient concentrations within the sediment column. In addition, data on the fraction of nutrients adsorbed on the sediment particles can help to understand the dynamics of porewater ammonium and SRP (Rocha, 1998; Sundareshwar & Morris, 1999).

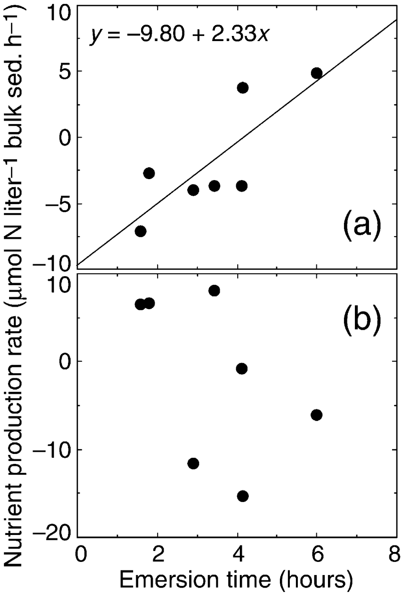

Fig. 8. Estimated nitrate (a) and ammonium (b) production rates (μmol N l^{-1} bulk sed. h^{-1}) (depth: 2.5–10 mm) versus emersion time. The estimated production rates were calculated by subtracting molecular diffusive fluxes from the observed rates of change in concentration (see Table 3). Negative values indicate the consumption of nutrients.

4.3. Nutrient dynamics at immersion

The concentration of interstitial nutrients changed markedly at immersion, however, with the exception of the decrease in nitrate and SRP in the surface layer, the concentration patterns were not simple (Fig. 6). For instance, in the topmost sediment sampled in May 1998, the concentration of nitrate and SRP decreased, but that of ammonium markedly increased. These complicated results relate partially to the low time resolution of the dynamics of each nutrient during the transitional tidal phase. Nevertheless, nitrate loss in surface sediments at immersion has also been reported by Rocha and Cabral (1998). They showed approximately 80% of the nitrate pool to be flushed at immersion of the Sado estuary. Similar results were reported for ammonium and SRP (Falcão & Vale, 1998; Rocha, 1998; Rocha, Cabeçadas, & Brogueira, 1995). Rocha et al. (1995) found that an abrupt rise in ammonium concentration occurred in the water column during the first hour of immersion in the Sado estuary. Falcão and Vale (1998) showed that during 20 min of immersion, large quantities of ammonium and SRP were transported to the overlying water in a coastal lagoon of Ria Formosa. Rocha (1998) reported that ~75% of total (dissolved and exchangeable) sedimentary ammonium was exported within 45 min of immersion.

Factors affecting solute dynamics during immersion can include (1) infiltration; (2) molecular diffusion; (3) external forces caused by tidal currents and waves; (4) free convention; and (5) bioturbation. The effect of infiltration is possibly not large for our case, because water content in the sediment did not change according to tidal regime. We calculated mass transport of interstitial nutrients occurred by molecular diffusion within the sediments (Diff(s)) and across the sediment–water interface (Diff(s–w)) (Table 4). The contribution of molecular diffusion to mass transport of nutrients after immersion in the top 10 mm sediments was minor for both Diff(s) (−2 to 26%, mean: 3.5%) and Diff(s–w) (−4 to 32%, mean: 9.2%). Therefore, the decrease in some interstitial nutrients in the surface layer cannot be explained by molecular diffusion alone. The external forces caused by tidal currents and waves can account for mixing of porewater with overlying water. de Jonge and van Beusekom (1995) speculated that the surface layer is more permeable as a result of hydrodynamic reworking. Inoue and Nakamura (2000) have shown theoretically that an abrupt increase in shear velocity can lead to a drastic increase in the SRP flux (1.7 times higher than steady state) at the sediment–water interface during the first 30 min of the experiment. They speculated that turbulent diffusion resulted in the rapid upward transport of accumulated SRP within the concentration boundary layer. In addition, Inoue and Nakamura (2000) found that a steep oxygen concentration increase in overlying water resulted in a change in the direction as well as the rate of SRP flux, due to enhancement of SRP adsorption by the sediment. Our complicated porewater nutrient dynamics at immersion may be partially explained by these externally controlled physico-chemical interactions. Free convection due to the temperature gradients within sediments, and between sediments and flooding water, can also promote mixing of porewater with overlying water (Rocha, 1998; Rocha & Cabral, 1998; Webster, Norquay, Ross, & Wooding, 1996). Many workers have suggested that macrofaunal reworking can cause much higher nutrient fluxes than molecular diffusion (e.g. Christensen, Vedel, & Kristensen, 2000; Kikuchi, 1986; Mortimer et al., 1999; Webster, 1992). The macrofaunal abundance at our site (Table 3), and associated enhanced bioturbation, would also increase nutrient efflux from the sediments.

All of the processes described above promote mixing of porewater with overlying water. Thus, in our case, mixing of low-nutrient overlying water (Fig. 4) with nutrient-rich porewater results in porewater nutrient

Table 4
Inventory of porewater nutrients (μmol N or P m^{-2}, depth: 0–10 mm) before (B) and after (A) immersion

		B	A	Diff(s)[a]	Diff(s)/A (%)	Diff(s–w)[b]	Diff(s–w)/A (%)	ΔI^c
$NO_3^- + NO_2^-$	March 1998	474	330	12	4	2	1	−130
	May 1998	305	98	25	26	7	7	−175
	September 1998	78	49	−1	−2	−2	−4	−32
	November 1998	220	229	6	3	32	14	47
NH_4^+	March 1998	626	538	0	0	6	1	−82
	May 1998	415	730	13	2	237	32	565
	September 1998	608	442	14	3	67	15	−85
	November 1998	192	227	1	0	36	16	72
PO_4^{3-}	March 1998	286	254	1	0	1	0	−30
	May 1998	224	126	2	2	7	6	−89
	September 1998	174	118	5	4	8	7	−43
	November 1998	109	114	1	1	18	16	24

[a] Diff(s), mass transport of porewater nutrients within the sediments occurred by molecular diffusion. Values are estimated as: diffusive flux calculated by Fick's second law of diffusion × time, where time is measured between the last sampling before immersion and the first sampling after immersion. Positive values indicate effluxes to the deeper layers.

[b] Diff(s–w), mass transport of porewater nutrients across the sediment–water interface occurred by molecular diffusion. Values are estimated as: diffusive flux calculated by Fick's first law of diffusion × time, where time is measured between immersion and the first sampling after immersion. Positive values indicate nutrient release from the sediments.

[c] Estimated as: A−(B−Diff(s)−Diff(s–w)).

depletion by dilution. Therefore, the increase in porewater ammonium for May 1998 is attributed to other mechanisms. These may include ongoing microbial reactions after emersion, and other mechanisms, such as stimulation of macrofaunal excretion during sediment reworking.

In summary, the water content in the surface sediment of the Banzu intertidal sandflat does not change significantly although a measurable decline in water table depth during emersion is found. Consequently, it is concluded that the influence of advective transport caused by a fluctuating water table on porewater nutrient dynamics is minor for our site. During emersion, both the production and diffusive flux of nutrient species greatly contribute to the observed rate of change in porewater nutrient concentration for the surface sediment. Microbial nitrate reduction within the subsurface sediment appears to be strongly fueled by downward diffusive flux of nitrate from the surface sediment. A promotion of estimated nitrate production rate proportional to the emersion time of the subsurface layer indicates a weakening of the anoxic environment by oxygenation during emersion, and subsequent stimulation of nitrification or inhibition of nitrate reduction. The marked decrease in interstitial nitrate and SRP concentrations in the surface layer at immersion cannot be explained by molecular diffusion alone.

Acknowledgements

We thank P.B. Christensen, Y. Uchiyama, A. Sohma, Y. Hosokawa and two anonymous reviewers for their helpful comments. We also thank E. Miyoshi for his kind help during fieldwork. This research was supported in part by a grant from the Ministry of the Environment, Japan.

References

Agosta, K. (1985). The effect of tidally induced changes in the creekbank water table on pore water chemistry. *Estuarine, Coastal and Shelf Science 21*, 389–400.

Allanson, B. R., Skinner, D., & Imberger, J. (1992). Flow in prawn burrows. *Estuarine, Coastal and Shelf Science 35*, 253–266.

Alongi, D. M. (1998). *Coastal ecosystem processes* (419 pp.). Boca Raton, FL: CRC Press.

Alongi, D. M., Tirendi, F., Dixon, P., Trott, L. A., & Brunskill, G. J. (1999). Mineralization of organic matter in intertidal sediments of a tropical semi-enclosed delta. *Estuarine, Coastal and Shelf Science 48*, 451–467.

Anderson, F. E., & Howell, B. A. (1984). Dewatering of an unvegetated muddy tidal flat during exposure—desiccation or drainage? *Estuaries 7*, 225–232.

Asmus, R. M., Jensen, M. H., Jensen, K. M., Kristensen, E., Asmus, H., & Wille, A. (1998). The role of water movement and spatial scaling for measurement of dissolved inorganic nitrogen fluxes in intertidal sediments. *Estuarine, Coastal and Shelf Science 46*, 221–232.

Berner, R. A. (1980). *Early diagenesis: A theoretical approach* (241 pp.). Princeton, NJ: Princeton University Press.

Brotas, V., Amorim-Ferreira, A., Vale, C., & Catarino, F. (1990). Oxygen profiles in intertidal sediments of Ria Formosa (S. Portugal). *Hydrobiologia 207*, 123–129.

Cabrita, M. T., & Brotas, V. (2000). Seasonal variation in denitrification and dissolved nitrogen fluxes in intertidal sediments of the Tagus estuary, Portugal. *Marine Ecology Progress Series 202*, 51–65.

Christensen, B., Vedel, A., & Kristensen, E. (2000). Carbon and nitrogen fluxes in sediment inhabited by suspension-feeding (*Nereis diversicolor*) and non-suspension-feeding (*N. Virens*) polychaetes. *Marine Ecology Progress Series 192*, 203–217.

Dolphin, T. J., Hume, T. M., & Parnell, K. E. (1995). Oceanographic processes and sediment mixing on a sand flat in an enclosed sea, Manukau Harbor, New Zealand. *Marine Geology 128*, 169–181.

Drabsch, J. M., Parnell, K. E., Hume, T. M., & Dolphin, T. J. (1999). The capillary fringe and the water table in an intertidal estuarine sand flat. *Estuarine, Coastal and Shelf Science 48*, 215–222.

Falcão, M., & Vale, C. (1990). Study of the Ria Formosa ecosystem: benthic nutrient remineralization and tidal variability of nutrients in the water. *Hydrobiologia 207*, 137–146.

Falcão, M., & Vale, C. (1998). Sediment–water exchanges of ammonium and phosphate in intertidal and subtidal areas of a mesotidal coastal lagoon (Ria Formosa). *Hydrobiologia 373/374*, 193–201.

Fenchel, T., King, G. M., & Blackburn, T. H. (1998). *Bacterial biogeochemistry: The ecophysiology of mineral cycling* (307 pp.). San Diego, CA: Academic Press.

Guo, X., & Yanagi, T. (1994). Three dimensional structure of tidal currents in Tokyo Bay, Japan. *La mer 32*, 173–185.

Harvey, J. W., & Odum, W. E. (1990). The influence of tidal marshes on upland groundwater discharge into estuaries. *Biogeochemistry 10*, 217–236.

Hemond, H. F., & Fifield, J. L. (1982). Subsurface flow in salt marsh peat: a model and field study. *Limnology and Oceanography 27*, 126–136.

Henriksen, K., & Kemp, W. M. (1988). Nitrification in estuarine and coastal marine sediments. In T. H. Blackburn, & J. Sørensen (Eds.), *Nitrogen cycling in coastal marine environments* (pp. 207–249). New York, NY: Wiley.

Howes, B. L., & Goehringer, D. D. (1994). Porewater drainage and dissolved organic carbon and nutrient losses through the intertidal creekbanks of a New England salt marsh. *Marine Ecology Progress Series 114*, 289–301.

Inoue, T., & Nakamura, Y. (2000). Response of sediment oxygen demand and phosphate release rate to a staircase change in DO concentration and flow velocity. *Journal of Hydroscience and Hydraulic Engineering 18*, 183–193.

de Jonge, V. N., & van Beusekom, J. E. E. (1995). Wind- and tide-induced resuspension of sediment and microphytobenthos from tidal flats in the Ems estuary. *Limnology and Oceanography 40*, 766–778.

Jørgensen, B. B., & Sørensen, J. (1985). Seasonal cycles of O_2, NO_3^- and SO_4^{2-} reduction in estuarine sediments: the significance of an NO_3^- reduction maximum in spring. *Marine Ecology Progress Series 24*, 65–74.

Kerner, M. (1993). Coupling of microbial fermentation and respiration processes in an intertidal mudflat of the Elbe estuary. *Limnology and Oceanography 38*, 314–330.

Kikuchi, E. (1986). Contribution of the polychaeta, *Neanthes japonica* (Izuka), to the oxygen uptake and carbon dioxide production of an intertidal mud-flat of the Nanakita River estuary. *Journal of Experimental Marine Biology and Ecology 97*, 81–93.

Koch, M. S., Maltby, E., Oliver, G. A., & Bakker, S. A. (1992). Factors controlling denitrification rates of tidal mudflats and fringing salt marshes in South-west England. *Estuarine, Coastal and Shelf Science 34*, 471–485.

Koike, I., & Sørensen, J. (1988). Nitrate reduction and denitrification in marine sediments: microbial activities and fluxes. In T. H. Blackburn, & J. Sørensen (Eds.), *Nitrogen cycling in coastal marine environments* (pp. 251–273). New York, NY: Wiley.

Kuwae, T., & Hosokawa, Y. (1999). Determination of abundance and biovolume of bacteria in sediments by dual staining with 4′,6-diamidino-2-phenylindole and acridine orange: relationship to dispersion treatment and sediment characteristics. *Applied and Environmental Microbiology 65*, 3407–3412.

Kuwae, T., Hosokawa, Y., & Eguchi, N. (1998). Dissolved inorganic nitrogen cycling in Banzu intertidal sand-flat, Japan. *Mangroves and Salt Marshes 2*, 167–175.

Li, Y. H., & Gregory, S. (1974). Diffusion of ions in sea water and deep-sea sediments. *Geochimica et Cosmochimica Acta 38*, 703–714.

Lorenzen, C. J. (1967). Determination of chlorophyll and pheopigments: spectrophotometric equations. *Limnology and Oceanography 12*, 343–346.

McLachlan, A., & Illenberger, W. (1986). Significance of groundwater nitrogen input to a beach/surf zone ecosystem. *Stygologia 2*, 291–296.

Middelburg, J. J., Klaver, G., Nieuwenhuize, J., & Vlug, T. (1995). Carbon and nitrogen cycling in intertidal sediments near Doel, Scheldt estuary. *Hydrobiologia 311*, 57–69.

Middelburg, J. J., Klaver, G., Nieuwenhuize, J., Wielemaker, A., de Haas, W., Vlug, T., & van der Nat, J. F. W. A. (1996). Organic matter mineralization in intertidal sediments along an estuarine gradient. *Marine Ecology Progress Series 132*, 157–168.

Mortimer, R. J. G., Davey, J. T., Krom, M. D., Watson, P. G., Frinkers, P. E., & Clifton, R. J. (1999). The effect of macrofauna on porewater profiles and nutrient fluxes in the intertidal zone of the Humber estuary. *Estuarine, Coastal and Shelf Science 48*, 683–699.

Nakanishi, H. (1993). Benthos. In N. Ogura (Ed.), *Tokyo Bay: Environmental changes in the past century* (pp. 77–101). Tokyo: Koseisha-Koseikaku (in Japanese).

Ottosen, L. D. M., Risgaard-Petersen, N., Nielsen, L. P., & Dalsgaard, T. (2001). Denitrification in exposed intertidal mud-flats, measured with a new ^{15}N-ammonium spray technique. *Marine Ecology Progress Series 209*, 35–42.

Parkin, T. B. (1990). Characterizing the variability of soil denitrification. In N. P. Revsbech, & J. Sørensen (Eds.), *Denitrification in soil and sediment* (pp. 213–228). New York, NY: Plenum Press.

Rocha, C. (1998). Rhythmic ammonium regeneration and flushing in intertidal sediments of the Sado estuary. *Limnology and Oceanography 43*, 823–831.

Rocha, C., Cabeçadas, G., & Brogueira, M. J. (1995). On the importance of sediment–water exchange processes of ammonia to primary production in shallow areas of the Sado estuary (Portugal). *Netherlands Journal of Aquatic Ecology 29*, 265–273.

Rocha, C., & Cabral, A. P. (1998). The influence of tidal action on porewater nitrate concentration and dynamics in intertidal sediments of the Sado estuary. *Estuaries 21*, 635–645.

Seitzinger, S. P. (1988). Denitrification in freshwater and coastal marine ecosystems: ecological and geochemical significance. *Limnology and Oceanography 33*, 702–724.

Strickland, J. D. H., & Parsons, T. R. (1972). *A practical handbook of seawater analysis* (2nd ed.), *Bulletin 167* (310 pp.). Ottawa: Fisheries Research Board of Canada.

Sundareshwar, P. V., & Morris, J. T. (1999). Phosphorus sorption characteristics of intertidal marsh sediments along an estuarine salinity gradient. *Limnology and Oceanography 44*, 1693–1701.

Sweerts, J. P. R. A., Kelly, C. A., Rudd, J. W. M., Hesslein, R., & Cappenberg, T. E. (1991). Similarity of whole-sediment molecular diffusion coefficients in freshwater sediments of low and high porosity. *Limnology and Oceanography 36*, 335–342.

Trimmer, M., Nedwell, D. B., Sivyer, D. B., & Malcolm, S. J. (2000). Seasonal benthic organic matter mineralisation measured by oxygen uptake and denitrification along a transect of the inner and outer River Thames estuary, UK. *Marine Ecology Progress Series 197*, 103–119.

Uchiyama, Y., Nadaoka, K., Rölke, P., Adachi, K., & Yagi, H. (2000). Submarine groundwater discharge into the sea and associated nutrient transport in a sandy beach. *Water Resources Research 36*, 1467–1479.

Usui, T., Koike, I., & Ogura, N. (1998). Tidal effect on dynamics of pore water nitrate in intertidal sediment of a eutrophic estuary. *Journal of Oceanography 54*, 205–216.

Webster, I. T. (1992). Wave enhancement of solute exchange within empty burrows. *Limnology and Oceanography 37*, 630–643.

Webster, I. T., Norquay, S. J., Ross, F. C., & Wooding, R. A. (1996). Solute exchange by convection within estuarine sediments. *Estuarine, Coastal and Shelf Science 42*, 171–183.

Yelverton, G. F., & Hackney, C. T. (1986). Flux of dissolved organic carbon and pore water through the substrate of a *Spartina alterniflora* marsh in North Carolina. *Estuarine, Coastal and Shelf Science 22*, 255–267.